

washed with brine and dried over MgSO_4 . Concentration under reduced pressure followed by recrystallization from *n*-hexane–EtOAc (10:1) gave the title compound **6** (1.03 g, 2.12 mmol, 96% yield) as colorless crystals: mp 145–146 °C; $[\alpha]_D^{25} +42.3$ (*c* 1.00, CHCl_3); IR (neat) 3372 (NH), 1707 (C=O); $^1\text{H NMR}$ (500 MHz, CDCl_3) δ 1.38 (s, 9H), 1.47 (s, 9H), 2.74 (dd, *J* = 14.3, 8.0 Hz, 1H), 2.89 (dd, *J* = 14.3, 6.9 Hz, 1H), 3.06 (s, 3H), 3.78 (s, 3H), 4.04–4.13 (m, 1H), 4.71 (d, *J* = 9.2 Hz, 1H), 5.18–5.24 (m, 1H), 6.02 (d, *J* = 15.5 Hz, 1H), 6.78 (dd, *J* = 15.5, 5.7 Hz, 1H), 6.84 (d, *J* = 8.6 Hz, 2H), 7.16 (d, *J* = 8.6 Hz, 2H); $^{13}\text{C NMR}$ (125 MHz, CDCl_3) δ 28.0 (3C), 28.2 (3C), 36.6, 39.2, 54.9, 55.2, 80.0, 80.3, 81.2, 114.0 (2C), 126.9, 128.5, 130.2 (2C), 139.2, 155.1, 158.5, 164.3. Anal. Calcd for $\text{C}_{23}\text{H}_{35}\text{NO}_8$: C, 56.89; H, 7.26; N, 2.88. Found: C, 56.96; H, 7.03; N, 2.85.

tert-Butyl (2*R*,5*R*,3*E*)-5-[*N*-(*tert*-Butoxycarbonyl)amino]-2-[3-(*tert*-butyldimethylsilyloxy)propyl]-6-(4-methoxyphenyl)hex-3-enoate (7). To a suspension of CuCN (1.79 g, 20.0 mmol) and LiCl (1.70 g, 40.0 mmol) in THF (40 mL) was added dropwise a solution of TBSO(CH_2)₃Li in *n*-pentane–Et₂O (0.5 M, 40.0 mL, 20.0 mmol) at –78 °C under argon, and the mixture was stirred for 30 min at 0 °C. To the above mixture was added dropwise a solution of the mesylate **6** (2.43 g, 5.0 mmol) in THF (20 mL) at –78 °C, and the mixture was stirred for 30 min at –78 °C. The reaction was quenched at –78 °C by the addition of a saturated $\text{NH}_4\text{Cl}/28\%$ NH_4OH solution (1:1, 50 mL), with additional stirring at room temperature for 3 h. After the mixture was concentrated under reduced pressure, the residue was extracted with Et₂O. The extract was washed with water and brine and dried over MgSO_4 . Concentration under reduced pressure followed by flash chromatography over silica gel with *n*-hexane–EtOAc (6:1) gave the title compound **7** (2.64 g, 4.68 mmol, 94% yield) as a colorless oil: $[\alpha]_D^{25} -14.9$ (*c* 1.09, CHCl_3); IR (neat) 3372 (NH), 1715 (C=O); $^1\text{H NMR}$ (500 MHz, CDCl_3) δ 0.04 (s, 6H), 0.89 (s, 9H), 1.28–1.48 (m, 21H), 1.66–1.75 (m, 1H), 2.62–2.87 (m, 3H), 3.56 (t, *J* = 6.3 Hz, 2H), 3.77 (s, 3H), 4.25–4.51 (m, 2H), 5.40–5.52 (m, 2H), 6.81 (d, *J* = 8.0 Hz, 2H), 7.09 (d, *J* = 8.0 Hz, 2H); $^{13}\text{C NMR}$ (125 MHz, CDCl_3) δ –5.4 (2C), 18.3, 25.9 (3C), 28.0 (3C), 28.3 (3C), 28.9, 30.0, 40.8, 49.5, 52.8, 55.1, 62.6, 79.2, 80.4, 113.7 (2C), 128.9, 129.4, 130.5 (2C), 132.1, 155.0, 158.2, 173.3; HRMS (FAB) *m/z* calcd for $\text{C}_{31}\text{H}_{54}\text{NO}_6\text{Si}$ (MH^+) 564.3715, found 564.3712.

tert-Butyl (2*R*,5*R*,3*E*)-2-[3-[*N*-[(Benzyloxy)carbonyl]-*N*-(2-nitrophenyl)sulfonylamino]propyl]-5-[*N*-(*tert*-butoxycarbonyl)amino]-6-(4-methoxyphenyl)hex-3-enoate (8). To a solution of the TBS ether **7** (2.59 g, 4.60 mmol) in MeCN–H₂O (1:1, 46 mL) was added aqueous H_2SiF_6 (3.28 M, 701 μL , 2.30 mmol) at 0 °C, and the mixture was stirred at room temperature for 2 h. After the mixture was concentrated, the residue was extracted with EtOAc. The extract was washed with 5% K_2CO_3 and brine and dried over MgSO_4 . Concentration under reduced pressure gave the corresponding alcohol, which was used in the next step without further purification. To a solution of the alcohol, PPh₃ (1.81 g, 6.90 mmol), and NsNH(Cbz) (1.70 g, 5.06 mmol) in THF (50 mL) was added diethyl azodicarboxylate (DEAD) in toluene (2.2 M, 2.51 mL, 5.52 mmol) at 0 °C under argon, and the mixture was stirred at the same temperature for 3 h. The reaction was quenched at 0 °C by the addition of MeOH (10 mL), with additional stirring at the same temperature for 30 min. Concentration under reduced pressure followed by flash chromatography over silica gel with *n*-hexane–EtOAc (3:1) gave the title compound **8** (3.03 g, 3.95 mmol, 86% yield) as a colorless oil: $[\alpha]_D^{25} -11.0$ (*c* 1.10, CHCl_3); IR (neat) 3411 (NH), 1720 (C=O); $^1\text{H NMR}$ (500 MHz, CDCl_3) δ 1.41 (s, 9H), 1.42 (s, 9H), 1.46–1.56 (m, 1H), 1.65–1.78 (m, 3H), 2.70–2.83 (m, 2H), 2.84–2.91 (m, 1H), 3.76 (s, 3H), 3.83 (t, *J* = 7.4 Hz, 2H), 4.21–4.61 (m, 2H), 5.10 (s, 2H), 5.43–5.53 (m, 2H), 6.82 (d, *J* = 8.6 Hz, 2H), 7.08 (d, *J* = 8.6 Hz, 2H), 7.18–7.23 (m, 2H), 7.29–7.36 (m, 3H), 7.41–7.47 (m, 1H), 7.62–7.71 (m, 2H), 8.09 (d, *J* = 8.0 Hz, 1H); $^{13}\text{C NMR}$ (125 MHz, CDCl_3) δ 27.4, 27.9 (3C), 28.3 (3C), 29.2, 40.6, 47.7, 49.2, 52.8, 55.1, 69.3, 79.1, 80.6, 113.6 (2C), 124.2, 128.4 (2C), 128.6 (2C), 128.7, 129.3, 130.0, 130.4, 130.5, 131.5, 132.4, 132.7, 134.0 (2C), 134.2, 147.6, 151.6, 155.0, 158.1, 172.8; HRMS (FAB) *m/z* calcd for $\text{C}_{39}\text{H}_{48}\text{N}_3\text{O}_{11}\text{S}$ (MH^-) 766.3015, found 766.3011.

tert-Butyl (2*R*,5*R*,3*E*)-2-[3-[*N*-[(Benzyloxy)carbonyl]amino]propyl]-5-[*N*-(*tert*-butoxycarbonyl)amino]-6-(4-methoxyphenyl)hex-3-enoate (9). To a stirred solution of enoate **8** (2.69 g, 3.50 mmol) in DMF (35 mL) were added thiophenol (715 μL , 7.00 mmol) and K_2CO_3 (1.45 g, 10.5 mmol) at room temperature, and the mixture was stirred at the same temperature for 3 h. After concentration under reduced pressure, the residue was extracted with EtOAc, washed with saturated citric acid, brine, 5% NaHCO_3 , and brine, and dried over MgSO_4 . Concentration under reduced pressure followed by flash chromatography over silica gel with *n*-hexane–EtOAc (3:1) gave the title compound **9** (1.95 g, 3.35 mmol, 96% yield) as a colorless oil: $[\alpha]_D^{25} -19.8$ (*c* 1.09, CHCl_3); IR (neat) 3342 (NH), 1700 (C=O); $^1\text{H NMR}$ (500 MHz, CDCl_3) δ 1.31–1.43 (m, 21H), 1.60–1.68 (m, 1H), 2.64–2.72 (m, 1H), 2.76–2.85 (m, 2H), 3.06–3.17 (m, 2H), 3.75 (s, 3H), 4.27–4.37 (m, 1H), 4.50–4.60 (m, 1H), 4.83–4.91 (m, 1H), 5.09 (s, 2H), 5.39–5.48 (m, 2H), 6.80 (d, *J* = 8.0 Hz, 2H), 7.06 (d, *J* = 8.0 Hz, 2H), 7.27–7.37 (m, 5H); $^{13}\text{C NMR}$ (125 MHz, CDCl_3) δ 27.2, 27.9 (3C), 28.3 (3C), 29.4, 40.6 (2C), 49.3, 52.9, 55.1, 66.5, 79.2, 80.6, 113.6 (2C), 127.96 (2C), 128.01, 128.4 (2C), 128.7, 129.4, 130.4 (2C), 132.4, 136.5, 155.0, 156.3, 158.1, 173.0; HRMS (FAB) *m/z* calcd for $\text{C}_{33}\text{H}_{45}\text{N}_2\text{O}_7$ (MH^-) 581.3232, found 581.3239.

(2*R*,5*R*,3*E*)-2-[3-[*N*-[(Benzyloxy)carbonyl]amino]propyl]-5-[*N*-(9-fluorenylmethoxy)carbonyl]amino]-6-(4-methoxyphenyl)hex-3-enoic Acid (10). To a stirred solution of enoate **9** (1.11 g, 1.90 mmol) in CH_2Cl_2 (20 mL) was added trifluoroacetic acid (5 mL), and the mixture was stirred for 2 h at room temperature. After concentration under reduced pressure, the residue was dissolved in water (10 mL). To this solution were added Et₃N (792 μL , 5.70 mmol) and FmocOSu (641 mg, 1.90 mmol) in MeCN (10 mL) at 0 °C, and the mixture was stirred for 2 h at room temperature. The reaction was quenched by addition of 1 N HCl. After concentration under reduced pressure, the residue was extracted with EtOAc. The extract was washed with 1 N HCl and brine and dried over MgSO_4 . Concentration under reduced pressure followed by flash chromatography over silica gel with *n*-hexane–EtOAc (1:1) containing 1% AcOH gave the title compound **10** (875 mg, 1.35 mmol, 71% yield) as colorless solids: mp 166–167 °C; $[\alpha]_D^{25} +1.7$ (*c* 1.09, DMSO); IR (neat) 1705 (C=O); $^1\text{H NMR}$ (500 MHz, $\text{DMSO}-d_6$) δ 1.26–1.46 (m, 3H), 1.52–1.69 (m, 1H), 2.70 (d, *J* = 6.9 Hz, 2H), 2.85–2.93 (m, 1H), 2.94–3.04 (m, 2H), 3.67 (s, 3H), 4.12–4.27 (m, 4H), 5.03 (s, 2H), 5.46 (dd, *J* = 15.5, 8.6 Hz, 1H), 5.57 (dd, *J* = 15.5, 5.7 Hz, 1H), 6.80 (d, *J* = 8.0 Hz, 2H), 7.13 (d, *J* = 8.0 Hz, 2H), 7.25–7.39 (m, 8H), 7.39–7.45 (m, 2H), 7.51 (d, *J* = 8.6 Hz, 1H), 7.63–7.71 (m, 2H), 7.88 (d, *J* = 7.4 Hz, 2H), 12.3 (s, 1H); $^{13}\text{C NMR}$ (125 MHz, $\text{DMSO}-d_6$) δ 27.0, 29.3, 40.0 (2C, overlapped with DMSO peaks), 46.7, 48.0, 54.2, 54.9, 65.2, 65.3, 113.5 (2C), 120.1 (2C), 125.3 (2C), 127.1 (2C), 127.6 (2C), 127.7 (2C), 127.7, 128.1, 128.4 (2C), 130.3 (2C), 130.4, 133.0 (2C), 137.3, 140.7 (2C), 143.9 (2C), 155.4, 156.2, 157.6, 175.0; HRMS (FAB) *m/z* calcd for $\text{C}_{39}\text{H}_{41}\text{N}_2\text{O}_7$ (MH^+) 649.2908, found 649.2921.

(3*R*,4*R*)-4-[*N*-(*tert*-Butoxycarbonyl)amino]-5-(4-methoxyphenyl)-3-methylpent-1-en-3-ol (12a). To a stirred solution of Boc-D-Phe-NMe(OMe) **11** (1.43 g, 4.23 mmol) in THF (35 mL) was added dropwise a solution of MeMgCl in THF (1.9 M, 6.7 mL, 12.7 mmol) at –78 °C under argon, and the mixture was stirred for 1.5 h at –78 °C. The reaction was quenched with saturated citric acid at –78 °C, and the whole was extracted with EtOAc. The extract was washed successively with saturated citric acid, brine, saturated NaHCO_3 , and brine and dried over MgSO_4 . Concentration under reduced pressure gave a crude ketone, which was used immediately in the next step without further purification. To a stirred suspension of anhydrous CeCl_3 (3.13 g, 12.7 mmol) and the above ketone in THF (30 mL) was added dropwise a solution of vinylmagnesium bromide in THF (1.3 M, 9.8 mL, 12.7 mmol) at 0 °C under argon. After 3 h, the reaction was quenched with saturated citric acid at –78 °C. The mixture was concentrated under reduced pressure and extracted with EtOAc. The extract was washed successively with saturated citric acid, brine, saturated NaHCO_3 , and brine and dried over Na_2SO_4 . Concentration under reduced pressure followed by flash chromatography over silica

gel with *n*-hexane–AcOEt (4:1) and recrystallization with *n*-hexane–AcOEt (10:1) gave the title compound **12a** (650 mg, 2.02 mmol, 48% yield) as white solids: mp 94–96 °C; $[\alpha]_D^{25} +78.2$ (*c* 0.98, CHCl₃); IR (neat) 3436 (NH), 1691 (C=O); ¹H NMR (500 MHz, CDCl₃) δ 1.28–1.37 (m, 12H), 2.50–2.60 (m, 1H), 2.90 (s, 1H), 3.04 (dd, *J* = 14.3, 3.4 Hz, 1H), 3.64–3.71 (m, 1H), 3.77 (s, 3H), 4.52 (d, *J* = 8.0 Hz, 1H), 5.15 (d, *J* = 10.3 Hz, 1H), 5.34 (d, *J* = 17.2 Hz, 1H), 5.98 (dd, *J* = 17.2, 10.3 Hz, 1H), 6.81 (d, *J* = 8.6 Hz, 2H), 7.09 (d, *J* = 8.6 Hz, 2H); ¹³C NMR (125 MHz, CDCl₃) δ 24.7, 28.2 (3C), 34.6, 55.3, 60.1, 75.7, 79.5, 113.3, 113.8 (2C), 130.0 (2C), 130.8, 142.8, 156.5, 158.1. Anal. Calcd for C₁₈H₂₇NO₄: C, 67.26; H, 8.47; N, 4.36. Found: C, 67.23; H, 8.49; N, 4.42.

(4*R*,5*R*)-*N*-(*tert*-Butoxycarbonyl)-5-ethenyl-4-(4-methoxybenzyl)-5-methyl-1,3-oxazolidin-2-one (13a). To a stirred suspension of NaH (1.64 g, 41.1 mmol) in THF (20 mL) was added dropwise a solution of the known allyl alcohol **12a** (3.30 g, 10.3 mmol) in THF (80 mL) at 0 °C under argon, and the mixture was heated under reflux for 1 h and stirred for 30 min at room temperature. (Boc)₂O (4.50 g, 20.6 mmol) was added to the mixture at 0 °C, and the mixture was stirred for 2 h with warming to room temperature. The mixture was poured into water at 0 °C, and the whole was extracted with EtOAc. The extract was washed successively with water and brine and dried over Na₂SO₄. Concentration under reduced pressure followed by flash chromatography over silica gel with *n*-hexane–EtOAc (6:1) gave the title compound **13a** (3.58 g, 10.3 mmol, quantitative) as white solids: mp 117–118 °C; $[\alpha]_D^{25} +82.3$ (*c* 1.02, CHCl₃); IR (neat) 1798 (C=O), 1714 (C=O); ¹H NMR (500 MHz, CDCl₃) δ 1.40 (s, 3H), 1.43 (s, 9H), 2.92 (dd, *J* = 14.3, 8.6 Hz, 1H), 3.06 (dd, *J* = 14.3, 5.7 Hz, 1H), 3.79 (s, 3H), 4.31 (dd, *J* = 8.6, 5.7 Hz, 1H), 5.16 (d, *J* = 10.9 Hz, 1H), 5.34 (d, *J* = 17.2 Hz, 1H), 5.76 (dd, *J* = 17.2, 10.9 Hz, 1H), 6.85 (d, *J* = 8.6 Hz, 2H), 7.15 (d, *J* = 8.6 Hz, 2H); ¹³C NMR (125 MHz, CDCl₃) δ 20.6, 27.8 (3C), 35.1, 55.2, 63.2, 82.1, 83.6, 114.2 (2C), 114.5, 128.5, 130.1 (2C), 139.5, 149.3, 151.4, 158.5. Anal. Calcd for C₁₉H₂₅NO₅: C, 65.69; H, 7.25; N, 4.03. Found: C, 65.40; H, 7.37; N, 4.03.

***tert*-Butyl (E)-3-[(4*R*,5*R*)-*N*-(*tert*-Butoxycarbonyl)-4-(4-methoxybenzyl)-5-methyl-1,3-oxazolidin-2-on-5-yl]prop-2-enoate (15a).** Ozone gas was bubbled into a stirred solution of the oxazolidin-2-one **13a** (211 mg, 0.61 mmol) in EtOAc (10 mL) at –78 °C until a blue color persisted. To the solution was added dimethyl sulfide (890 μL, 12.2 mmol) at –78 °C, and the mixture was stirred for 0.5 h at –78 °C. The mixture was dried over Na₂SO₄ and concentrated under reduced pressure to give the corresponding aldehyde, which was used for the next reaction without further purification. To a stirred suspension of LiCl (52.0 mg, 1.22 mmol) in MeCN (4.0 mL) were added *tert*-butyl diethylphosphonoacetate (380 μL, 1.22 mmol) and (*i*-Pr)₂NEt (213 μL, 1.22 mmol) successively at 0 °C under argon. After 30 min, the above aldehyde in MeCN (2.0 mL) was added to the mixture at 0 °C, and the stirring was continued for 3.5 h. The reaction was quenched by addition of saturated NH₄Cl. After concentration under reduced pressure, the residue was extracted with EtOAc. The extract was washed with saturated citric acid, brine, saturated NaHCO₃, and brine and dried over Na₂SO₄. Concentration under reduced pressure followed by flash chromatography over silica gel with *n*-hexane–EtOAc (4:1) gave the title compound **15a** (152 mg, 0.34 mmol, 56% yield) as white solids: mp 140–141 °C; $[\alpha]_D^{26} +92.8$ (*c* 0.99, CHCl₃); IR (neat) 1800 (C=O), 1714 (C=O); ¹H NMR (500 MHz, CDCl₃) δ 1.42 (s, 3H), 1.47 (s, 18H), 2.94 (dd, *J* = 14.3, 9.2 Hz, 1H), 3.12 (dd, *J* = 14.3, 4.6 Hz, 1H), 3.80 (s, 3H), 4.37 (dd, *J* = 9.2, 4.6 Hz, 1H), 6.00 (d, *J* = 16.0 Hz, 1H), 6.63 (d, *J* = 16.0 Hz, 1H), 6.86 (d, *J* = 8.0 Hz, 2H), 7.15 (d, *J* = 8.0 Hz, 2H); ¹³C NMR (125 MHz, CDCl₃) δ 20.5, 27.8 (3C), 28.0 (3C), 34.9, 55.2, 62.8, 81.2, 81.3, 84.2, 114.3 (2C), 122.6, 128.0, 130.0 (2C), 146.1, 149.0, 150.9, 158.6, 165.0. Anal. Calcd for C₂₄H₃₃NO₇: C, 64.41; H, 7.43; N, 3.13. Found: C, 64.48; H, 7.23; N, 3.10.

***tert*-Butyl (2*R*,5*R*,3*E*)-5-[*N*-(*tert*-Butoxycarbonyl)amino]-2-(3-hydroxypropyl)-6-(4-methoxyphenyl)-4-methylhex-3-enoate (17a).** To a solution of the TBS ether **16a** (52.6 mg, 0.091 mmol) in MeCN–H₂O (1:1, 2.0 mL) was added aqueous H₂SiF₆ (3.28 M, 28 μL, 0.091 mmol) at room temperature, and the mixture was stirred for

14 h. The reaction was quenched by addition of saturated NH₄Cl. After concentration under reduced pressure, the residue was extracted with EtOAc. The extract was washed with saturated NH₄Cl, brine, saturated NaHCO₃, and brine and dried over Na₂SO₄. Concentration under reduced pressure followed by flash chromatography over silica gel with *n*-hexane–EtOAc (1:1) gave the title compound **17a** (21.7 mg, 0.047 mmol, 51% yield) as a colorless oil: $[\alpha]_D^{25} -37.3$ (*c* 1.03, CHCl₃); IR (neat) 1699 (C=O); ¹H NMR (500 MHz, CDCl₃) δ 1.28–1.34 (m, 3H), 1.37–1.41 (m, 10H), 1.42 (s, 9H), 1.62–1.70 (m, 4H), 2.76 (d, *J* = 6.9 Hz, 2H), 3.03–3.12 (m, 1H), 3.51 (t, *J* = 6.9 Hz, 2H), 3.77 (s, 3H), 4.09–4.31 (m, 1H), 4.64 (d, *J* = 8.0 Hz, 1H), 5.16 (d, *J* = 9.2 Hz, 1H), 6.80 (d, *J* = 8.6 Hz, 2H), 7.05 (d, *J* = 8.6 Hz, 2H); ¹³C NMR (125 MHz, CDCl₃) δ 14.3, 28.0 (3C), 28.3 (3C), 28.7, 29.9, 38.8, 45.1, 55.2, 58.2, 62.4, 79.3, 80.4, 113.7 (2C), 124.5, 129.8, 130.1 (2C), 136.9, 155.0, 158.1, 173.5; HRMS (FAB) *m/z* calcd for C₂₆H₄₂NO₆ (MH⁺) 464.3007, found 464.3010.

***tert*-Butyl (2*R*,5*R*,3*E*)-2-[3-[*N*-[(Benzoyloxy)carbonyl]-*N*-[(2-nitrophenyl)sulfonyl]amino]propyl]-5-[*N*-(*tert*-butoxycarbonyl)amino]-6-(4-methoxyphenyl)-4-methylhex-3-enoate (18a).** To a solution of the alcohol **17a** (21.7 mg, 0.047 mmol), PPh₃ (24.6 mg, 0.094 mmol), and NsNH(Cbz) (33.0 mg, 0.094 mmol) in THF (0.47 mL) was added DEAD in toluene (2.2 mL, 43 μL, 0.094 mmol) at 0 °C under argon, and the mixture was stirred at the same temperature overnight. Concentration under reduced pressure followed by flash chromatography over silica gel with *n*-hexane–EtOAc (3:1) gave the title compound **18a** (22.4 mg, 0.029 mmol, 61% yield) as a yellow oil: $[\alpha]_D^{25} -24.0$ (*c* 1.02, CHCl₃); IR (neat) 1726 (C=O); ¹H NMR (500 MHz, CDCl₃) δ 1.38 (s, 9H), 1.40–1.48 (m, 10H), 1.57–1.78 (m, 6H), 2.69–2.85 (m, 2H), 3.06–3.18 (m, 1H), 3.77 (s, 3H), 3.80 (t, *J* = 7.4 Hz, 2H), 4.12–4.28 (m, 1H), 4.50–4.67 (m, 1H), 5.11 (s, 2H), 5.19 (d, *J* = 9.7 Hz, 1H), 6.80 (d, *J* = 8.6 Hz, 2H), 7.06 (d, *J* = 8.6 Hz, 2H), 7.17–7.25 (m, 2H), 7.29–7.40 (m, 3H), 7.41–7.51 (m, 1H), 7.61–7.76 (m, 2H), 8.10 (d, *J* = 8.0 Hz, 1H); ¹³C NMR (125 MHz, CDCl₃) δ 14.3, 27.4, 27.9 (3C), 28.3 (3C), 29.4, 39.0, 45.0, 47.9, 55.2, 58.0, 69.3, 79.1, 80.4, 113.7 (2C), 124.2, 124.3, 128.5 (2C), 128.6 (2C), 128.7, 129.8, 130.1 (2C), 131.5, 132.8, 134.09, 134.11, 134.2, 137.5, 147.7, 151.6, 155.0, 158.1, 173.0; HRMS (FAB) *m/z* calcd for C₄₀H₅₂N₃O₁₁S (MH⁺) 782.3317, found 782.3319.

(4*R*,5*S*)-5-Acetyl-*N*-(*tert*-butoxycarbonyl)-4-(4-methoxybenzyl)-5-methyl-1,3-oxazolidin-2-one (14). Ozone gas was bubbled into a stirred solution of the oxazolidin-2-one **13b** (1.20 g, 3.32 mmol) in EtOAc (40 mL) at –78 °C until a blue color persisted. To the solution was added dimethyl sulfide (2.4 mL, 33.2 mmol) at –78 °C, and the mixture was stirred for 15 min at –78 °C. Concentration under reduced pressure followed by flash chromatography over silica gel with *n*-hexane–EtOAc (2:1) gave the title compound **14** (1.19 g, 3.28 mmol, 99% yield) as colorless crystals: mp 91–92 °C; $[\alpha]_D^{26} +48.0$ (*c* 1.02, CHCl₃); IR (neat) 1817 (C=O), 1725 (C=O); ¹H NMR (500 MHz, CDCl₃) δ 1.35 (s, 3H), 1.44 (s, 9H), 2.28 (s, 3H), 2.93 (dd, *J* = 14.9, 8.6 Hz, 1H), 3.05 (dd, *J* = 14.3, 5.2 Hz, 1H), 3.79 (s, 3H), 4.86 (dd, *J* = 8.6, 5.2 Hz, 1H), 6.85 (d, *J* = 8.6 Hz, 2H), 7.16 (d, *J* = 8.6 Hz, 2H); ¹³C NMR (125 MHz, CDCl₃) δ 17.6, 24.8, 27.8 (3C), 34.8, 55.2, 60.0, 84.3, 86.5, 114.3 (2C), 127.7, 130.0 (2C), 148.4, 150.4, 158.6, 207.8. Anal. Calcd for C₁₉H₂₅NO₆: C, 62.80; H, 6.93; N, 3.85. Found: C, 62.68; H, 6.80; N, 3.89.

***tert*-Butyl (E)-3-[(4*R*,5*R*)-*N*-(*tert*-Butoxycarbonyl)-4-(4-methoxybenzyl)-5-methyl-1,3-oxazolidin-2-on-5-yl]but-2-enoate (15b).** The ketone **14** (490 mg, 1.35 mmol) and Ph₃P=CHCO₂-*t*-Bu (1.11 g, 2.97 mmol) were dissolved in toluene (6.0 mL), and the mixture was gently refluxed for 10 h. Concentration under reduced pressure followed by flash chromatography over silica gel with *n*-hexane–EtOAc (3:1) gave the title compound **15b** (621 mg, 1.35 mmol, quantitative) as colorless crystals: mp 174–175 °C; $[\alpha]_D^{26} +76.7$ (*c* 1.00, CHCl₃); IR (neat) 1813 (C=O), 1714 (C=O); ¹H NMR (500 MHz, CDCl₃) δ 1.41 (s, 3H), 1.46 (s, 9H), 1.49 (s, 9H), 1.91 (d, *J* = 1.2 Hz, 3H), 2.94 (dd, *J* = 14.3, 9.2 Hz, 1H), 3.12 (dd, *J* = 14.3, 4.6 Hz, 1H), 3.80 (s, 3H), 4.42 (dd, *J* = 9.2, 4.6 Hz, 1H), 5.95 (d, *J* = 1.2 Hz, 1H), 6.87 (d, *J* = 8.6 Hz, 2H), 7.18 (d, *J* = 8.6 Hz, 2H); ¹³C NMR (125 MHz, CDCl₃) δ 14.7, 20.2, 27.9 (3C), 28.1 (3C), 35.3, 55.2,

61.5, 80.5, 84.2, 84.4, 114.3 (2C), 117.1, 128.1, 130.1 (2C), 149.0, 150.6, 153.9, 158.6, 165.7. Anal. Calcd for $C_{25}H_{35}NO_7$: C, 65.06; H, 7.64; N, 3.03. Found: C, 64.97; H, 7.71; N, 3.07.

tert-Butyl (Z)-3-[(4R,5R)-N-(tert-Butoxycarbonyl)-4-(4-methoxybenzyl)-5-methyl-1,3-oxazolidin-2-on-5-yl]but-2-enoate (21). To a solution of diisopropylamine (41.0 μ L, 0.29 mmol) in THF (0.29 mL) at -78°C was added dropwise *n*-BuLi in *n*-hexane (1.65 M, 0.18 mL, 0.29 mmol). After the mixture was stirred at 0°C for 30 min, a solution of $\text{TMSCH}_2\text{CO}_2$ -*t*-Bu (66.0 μ L, 0.30 mmol) in THF (0.19 mL) was added dropwise at -78°C . After the mixture was stirred at -78°C for 2 h, a solution of ketone **14** (21.0 mg, 0.058 mmol) in THF (0.19 mL) was added dropwise. The resulting mixture was stirred at -78°C for 4 h. The reaction was quenched by addition of saturated NH_4Cl at -78°C . The whole mixture was stirred at room temperature for 15 min, extracted with Et_2O , and dried over MgSO_4 . Concentration under reduced pressure followed by flash chromatography over silica gel with *n*-hexane– EtOAc (3:1) gave an *E/Z* mixture of the title compound **21** and **15b** (14.2 mg, 0.031 mmol, 53% yield, **15b/21** = 3/2) as a clear oil. Data for compound **21** (purified by preparative HPLC): colorless oil; $[\alpha]_D^{25}$ -115.7 (*c* 1.01, CHCl_3); IR (neat) 1818 ($\text{C}=\text{O}$), 1705 ($\text{C}=\text{O}$); ^1H NMR (500 MHz, $\text{DMSO}-d_6$) δ 1.16 (s, 9H), 1.52 (s, 9H), 1.73 (s, 3H), 1.94 (d, *J* = 1.7 Hz, 3H), 2.66 (dd, *J* = 13.7, 10.3 Hz, 1H), 3.30 (dd, *J* = 13.7, 3.4 Hz, 1H), 3.77 (s, 3H), 4.76 (dd, *J* = 10.3, 3.4 Hz, 1H), 5.74 (d, *J* = 1.7 Hz, 1H), 6.82 (d, *J* = 8.6 Hz, 2H), 7.14 (d, *J* = 8.6 Hz, 2H); ^{13}C NMR (125 MHz, $\text{DMSO}-d_6$) δ 19.2, 22.7, 27.4 (3C), 28.1 (3C), 36.2, 55.2, 65.2, 80.7, 82.9, 85.9, 114.0 (2C), 119.0, 129.0, 130.7 (2C), 148.7, 151.6, 158.5, 160.8, 164.7; HRMS (FAB) *m/z* calcd for $C_{25}H_{36}NO_7$ (MH^+) 462.2486 found 462.2486.

Peptide Synthesis. The protected linear peptides **28a–c** were constructed by Fmoc-based solid-phase synthesis on H-Gly-(2-Cl)Trt resin (0.66 mmol/g, 152 mg, 0.10 mmol). The Pbf group for Arg was employed for side chain protection. Fmoc-protected amino acids (0.30 mmol) were coupled by using *N,N'*-diisopropylcarbodiimide (DIC) (46.4 μ L, 0.3 mmol) and $\text{HOBT}\cdot\text{H}_2\text{O}$ (45.9 mg, 0.3 mmol) in DMF. Coupling of dipeptide isostere **10**, **20a**, or **20b** (0.30 mmol) was carried out with DIC (46.4 μ L, 0.3 mmol) and HOAt (40.8 mg, 0.30 mmol). Completion of each coupling reaction was ascertained using the Kaiser ninhydrin test. The Fmoc protecting group was removed by treating the resin with 20% piperidine in DMF.

By use of a procedure identical with that described for the preparation of the protected linear peptide, **28d** was obtained from H-Gly-(2-Cl)Trt resin (0.80 mmol/g, 125 mg, 0.10 mmol) using dipeptide isostere **26** (0.30 mmol).

Cyclo(D-Tyr- ψ [(E)-CH=CH]-Arg-Arg-Nal-Gly)-2TFA (31a). The resulting protected peptide resin **28a** (275 mg) was subjected to hexafluoro-2-propanol (HFIP)– CH_2Cl_2 (2:8, 15 mL) treatment at room temperature for 2 h. After filtration of the residual resin, the filtrate was concentrated under reduced pressure to give a crude linear peptide, **29a**. To a mixture of the linear peptide and NaHCO_3 (42.0 mg, 0.500 mmol) in DMF (40 mL) was added diphenylphosphoryl azide (DPPA; 53.9 μ L, 0.250 mmol) at -40°C . The mixture was stirred for 40 h with warming to room temperature and then filtered. The filtrate was concentrated under reduced pressure, followed by flash chromatography over silica gel with CHCl_3 –MeOH (90:10) to give the protected cyclic peptide **30a**. The peptide **30a** was treated with 1 M TMSOTf–thioanisole in TFA (3 mL) at room temperature for 3 h. Concentration under reduced pressure gave an oily residue, which was used immediately in the next step without purification. To a solution of the crude mixture in DMF (2 mL) were added (*i*-Pr) $_2\text{NEt}$ (261 μ L, 1.50 mmol) and 1*H*-pyrazole-1-carboxamide hydrochloride (73.3 mg, 0.500 mmol), and the mixture was stirred at room temperature for 2 days. After concentration under reduced pressure, purification by preparative HPLC gave the bistrifluoroacetate of the title cyclic peptide **31a** (20.4 mg, 0.0217 mmol, 22% yield based on H-Gly-(2-Cl)Trt resin) as a colorless freeze-dried powder: $[\alpha]_D^{28}$ -43.4 (*c* 0.133, DMSO); ^1H NMR (500 MHz, $\text{DMSO}-d_6$) δ 1.25–1.50 (m, 5H), 1.52–1.70 (m, 3H), 2.58 (d, *J* = 7.6 Hz, 2H), 2.74 (ddd, *J* = 8.2, 8.2, 7.6 Hz, 1H), 2.94–3.15 (m, 6H), 3.29 (dd, *J* = 15.8, 5.5 Hz, 1H), 3.66 (dd, *J* = 15.8, 6.9 Hz, 1H), 4.14 (ddd, *J* = 8.9, 8.2, 8.2 Hz, 1H),

4.32–4.41 (m, 1H), 4.53 (ddd, *J* = 7.6, 7.6, 6.9 Hz, 1H), 5.39 (ddd, *J* = 15.1, 8.9, 1.4 Hz, 1H), 5.55 (dd, *J* = 15.1, 4.1 Hz, 1H), 6.62 (d, *J* = 8.3 Hz, 2H), 6.93 (d, *J* = 8.3 Hz, 2H), 7.02 (d, *J* = 8.3 Hz, 1H), 7.30 (dd, *J* = 8.3, 2.1 Hz, 1H), 7.42–7.50 (m, 2H), 7.50–7.57 (m, 2H), 7.61 (s, 1H), 7.76 (d, *J* = 8.9 Hz, 1H), 7.79–7.87 (m, 4H), 8.35 (dd, *J* = 6.9, 5.5 Hz, 1H), 9.15 (s, 1H); ^{13}C NMR (125 MHz, $\text{DMSO}-d_6$) δ 25.3, 26.3, 27.9, 28.4, 29.0, 38.1, 40.1 (overlapped with DMSO peaks), 40.3, 43.5, 50.3, 51.5, 54.3, 54.5, 115.0 (2C), 125.5, 126.0, 127.4, 127.4, 127.5, 127.6, 127.66, 127.75, 128.0, 130.1 (2C), 131.9, 132.8, 132.9, 134.8, 155.6, 156.72, 156.75, 167.6, 170.6, 171.5, 172.2; HRMS (FAB) *m/z* calcd for $C_{37}H_{49}N_{10}O_5$ (MH^+) 713.3882, found 713.3881.

Cyclo(D-Tyr- ψ [-CH $_2$ -CH $_2$]-Arg-Arg-Nal-Gly)-2TFA (31e). The cyclic pseudopeptide **31a** (2.64 mg, 0.0281 mmol) was treated with Pd/BaSO $_4$ (59.5 mg, 0.0281 mmol) in MeOH (300 μ L) under a H_2 atmosphere at room temperature for 36 h. After filtration and concentration under reduced pressure, purification by preparative HPLC gave the bistrifluoroacetate of the title peptide **31e** (0.874 mg, 0.00927 mmol, 33% yield) as a colorless freeze-dried powder: $[\alpha]_D^{29}$ -31.7 (*c* 0.0933, DMSO); ^1H NMR (500 MHz, $\text{DMSO}-d_6$) δ 1.08–1.53 (m, 10H), 1.61–1.79 (m, 2H), 1.91–2.04 (m, 1H), 2.35 (dd, *J* = 13.2, 7.4 Hz, 1H), 2.46–2.58 (m, 1H, overlapped with DMSO peak), 2.95–3.10 (m, 4H), 3.14 (dd, *J* = 13.7, 9.7 Hz, 1H), 3.24 (dd, *J* = 13.7, 4.6 Hz, 1H), 3.44–3.48 (m, 1H), 3.61–3.72 (m, 1H), 3.75–3.84 (m, 1H), 3.84–3.93 (m, 1H), 4.42–4.52 (m, 1H), 6.45 (d, *J* = 9.7 Hz, 1H), 6.62 (d, *J* = 8.0 Hz, 2H), 6.89 (d, *J* = 8.0 Hz, 2H), 7.41–7.56 (m, 5H), 7.76 (s, 1H), 7.82–7.90 (m, 3H), 8.10 (d, *J* = 7.4 Hz, 1H), 8.13–8.21 (m, 1H), 8.26–8.36 (m, 1H), 9.14 (s, 1H); ^{13}C NMR (125 MHz, $\text{DMSO}-d_6$) δ 25.4, 26.5, 27.0, 29.0, 29.3, 31.2, 36.4, 40.2, 40.4, 41.2, 42.5, 46.9, 50.4, 53.7, 56.1, 115.0 (2C), 125.5, 126.1, 127.2, 127.4, 127.47, 127.55, 127.8, 128.7, 129.9 (2C), 131.8, 133.0, 135.6, 155.5, 156.68, 156.70, 168.0, 170.7, 172.6, 174.8; HRMS (FAB) *m/z* calcd for $C_{37}H_{51}N_{10}O_5$ (MH^+) 715.4038, found 715.4046.

[^{125}I]SDF-1 Binding and Displacement. Membrane extracts were prepared from HEK293 cell lines expressing CXCR4. For ligand binding, 50 μ L of the inhibitor, 25 μ L of [^{125}I]SDF-1 α (0.3 nM, Perkin-Elmer Life Sciences), and 25 μ L of the membrane/ bead mixture [7.5 μ g of membrane/well, 0.5 mg of PVT WGA beads (Amersham)/well] in assay buffer (25 mM HEPES, pH 7.4, 1 mM CaCl_2 , 5 mM MgCl_2 , 140 mM NaCl, 250 mM sucrose, 0.5% BSA) were incubated in the wells of an Optiplate plate (Perkin-Elmer Life Sciences) at room temperature for 1 h. The bound radioactivity was counted for 1 min/well in a TopCount (Packard). The inhibitory activity of the test compounds was determined on the basis of the inhibition of [^{125}I]SDF-1 binding to the receptors (IC_{50} , triplicate experiments, Table 1).

NMR Spectroscopy. The peptide sample was dissolved in $\text{DMSO}-d_6$ at 5 mM. ^1H NMR spectra of the peptides were recorded at 300 K. The assignment of the proton resonance was achieved by use of ^1H – ^1H COSY spectra. COSY spectra were composed of 2048 complex points in the F_2 dimension and 256 complex points, which were zero-filled to yield a final data matrix of 2048 \times 512 points. $^3\text{J}(\text{H}^N, \text{H}^\alpha)$ coupling constants were measured from one-dimensional spectra. The mixing time for NOESY experiments was set at 200 ms. NOESY spectra were composed of 1024 complex points in the F_2 dimension and 512 complex points, which were zero-filled to yield a final data matrix of 1024 \times 1024 points, with 32 scans per t_1 increment. The cross-peak intensities were classified on the basis of the number of contour lines.

Structural Calculations. The structure calculations were performed by MacroModel using the MMFFs. Pseudoatoms were defined for the CH_3 protons on the alkene of **31b–d**, methylene protons of D-Tyr 1 , D/L-Arg 2 , L-Arg 3 , and L-Nal 4 , and aromatic protons of D-Tyr 1 , the prochiralities of which were not identified from ^1H NMR data. The dihedral φ angle constraints were calculated on the basis of the Karplus equation: $^3\text{J}(\text{H}^N, \text{H}^\alpha) = 6.7 \cos^2 \theta - 1.3 \cos \theta + 1.5$. Lower and upper angle errors were set to 15° . The NOESY spectrum with a mixing time of 200 ms was used for the estimation of the distance restraints between protons. The NOE intensities were classified into three categories (strong, medium, and weak) on the basis of the number of contour lines in the cross-peaks to define the

upper limit distance restraints (2.7, 3.5, and 5.0 Å, respectively). The upper limit restraints were increased by 1.0 Å for the involved pseudoatoms except the aromatic protons, for which the restraints were increased by 2.0 Å. Lower bounds between nonbonded atoms were set to their van der Waals radii (1.8 Å). A total of 100 000 random structures were generated by molecular dynamic simulation starting with any initial structure in water; the structures matched with the restraints from the NMR data were then selected. The structure in the lowest potential energy was defined as the most stable structure in solution.

Docking of Peptidomimetics to CXCR4. Initial structures of 31a–c, 31d-A, and 31d-B were built by energy minimization of NMR-based structures described above. The resulting models were incorporated into CXCR4, and the water molecules of the crystal structure of CXCR4 bound to CVX15 (PDB code 3OE0) were manually input as appropriate. After that, the structures of peptidomimetics were minimized in the receptor structure in MOE using MMFF94s and a distance-dependent dielectric constant of 1 with a 10 Å cutoff distance. The steepest descent algorithm was used for the minimization, followed by the conjugate gradient method. The maximum iterations of each run were set to 100 steps, and the root-mean-square (rms) gradient value of 0.01 was set for the criteria of the minimizations. In this calculation, the backbone atoms of the receptor were fixed.

■ ASSOCIATED CONTENT

Supporting Information

Experimental procedures and characterization data for all new compounds. This material is available free of charge via the Internet at <http://pubs.acs.org>.

■ AUTHOR INFORMATION

Corresponding Author

*Phone: +81-75-753-4551. Fax: +81-75-753-4570. E-mail: soishi@pharm.kyoto-u.ac.jp (S.O.); nfujii@pharm.kyoto-u.ac.jp (N.F.).

Notes

The authors declare no competing financial interest.

■ ACKNOWLEDGMENTS

This work was supported by Grants-in-Aid for Scientific Research and the Targeted Protein Research Program from MEXT and Health and Labor Science Research Grants (Research on HIV/AIDS, Japan). K.K. and K.T. are grateful for JSPS Research Fellowships for Young Scientists.

■ ABBREVIATIONS USED

CXCR4, CXC chemokine receptor type 4; HWE reaction, Horner–Wadsworth–Emmons reaction; HIV, human immunodeficiency virus; MMFFs, Merck molecular force field; MOE, Molecular Operating Environment; Nal, 3-(2-naphthyl)alanine; Orn, ornithine; SAR, structure–activity relationship; SDF-1, stromal-cell-derived factor-1

■ REFERENCES

- (1) Fung, S.; Hruby, V. J. Design of cyclic and other templates for potent and selective peptide α -MSH analogues. *Curr. Opin. Chem. Biol.* **2005**, *9*, 352–358.
- (2) Mosberg, H. L.; Hurst, R.; Hruby, V. J.; Gee, K.; Yamaura, H. I.; Galligan, J. J.; Burks, T. F. Bis-penicillamine enkephalins possess highly improved specificity toward δ opioid receptors. *Proc. Natl. Acad. Sci. U.S.A.* **1983**, *80*, 5871–5874.
- (3) March, D. R.; Abbenante, G.; Bergman, D. A.; Brinkworth, R. L.; Wickramasinghe, W.; Begun, J.; Martin, J. L.; Fairlie, D. P. Substrate-based cyclic peptidomimetics of Phe-Ile-Val that inhibit HIV-1

protease using a novel enzyme-binding mode. *J. Am. Chem. Soc.* **1996**, *118*, 3375–3379.

- (4) Burton, P. S.; Conradi, R. A.; Ho, N. F. H.; Hilgers, A. R.; Borchardt, R. T. How structural features influence the biomembrane permeability of peptides. *J. Pharm. Sci.* **1996**, *85*, 1336–1340.

- (5) Rezai, T.; Yu, B.; Millhauser, G. L.; Jacobson, M. P.; Lokey, R. S. Testing the conformational hypothesis of passive membrane permeability using synthetic cyclic peptide diastereomers. *J. Am. Chem. Soc.* **2006**, *128*, 2510–2511.

- (6) Kessler, H. Conformation and biological activity of cyclic peptides. *Angew. Chem., Int. Ed. Engl.* **1982**, *21*, 512–523.

- (7) Aumailley, M.; Gurrath, M.; Müller, G.; Calvete, J.; Timpl, R.; Kessler, H. Arg-Gly-Asp constrained within cyclic pentapeptides. Strong and selective inhibitors of cell adhesion to vitronectin and laminin fragment P1. *FEBS Lett.* **1991**, *291*, 50–54.

- (8) Dechantsreiter, M. A.; Planker, E.; Mathä, B.; Lohof, E.; Hölzemann, G.; Jonczyk, A.; Goodman, S. L.; Kessler, H. N-Methylated cyclic RGD peptides as highly active and selective $\alpha_v\beta_3$ integrin antagonists. *J. Med. Chem.* **1999**, *42*, 3033–3040.

- (9) Haubner, R.; Gratias, R.; Diefenbach, B.; Goodman, S. L.; Jonczyk, A.; Kessler, H. Structural and functional aspects of RGD-containing cyclic pentapeptides as highly potent and selective integrin $\alpha_v\beta_3$ antagonists. *J. Am. Chem. Soc.* **1996**, *118*, 7461–7472.

- (10) Keenan, R. M.; Miller, W. H.; Kwon, C.; Ali, F. E.; Callahan, J. F.; Calvo, R. R.; Hwang, S. M.; Kopple, K. D.; Peishoff, C. E.; Samanen, J. M.; Wong, A. S.; Yuan, C. K.; Huffman, W. F. Discovery of potent nonpeptide vitronectin receptor ($\alpha_v\beta_3$) antagonists. *J. Med. Chem.* **1997**, *40*, 2289–2292.

- (11) Nicolaou, K. C.; Trujillo, J. I.; Jandeleit, B.; Chibale, K.; Rosenfeld, M.; Diefenbach, B.; Cheresch, D. A.; Goodman, S. L. Design, synthesis and biological evaluation of nonpeptide integrin antagonists. *Bioorg. Med. Chem.* **1998**, *6*, 1185–1208.

- (12) Rockwell, A. L.; Rafalski, M.; Pitts, W. J.; Batt, D. G.; Petraitis, J. J.; DeGrado, W. F.; Mousa, S.; Jadhav, P. K. Rapid synthesis of RGD mimetics with isoxazoline scaffolds on solid phase: identification of $\alpha_v\beta_3$ antagonists lead compounds. *Bioorg. Med. Chem. Lett.* **1999**, *9*, 937–942.

- (13) Ihara, M.; Noguchi, K.; Saeki, T.; Fukuroda, T.; Tsuchida, S.; Kimura, S.; Fukami, T.; Ishikawa, K.; Nishikibe, M.; Yano, M. Biological profiles of highly potent novel endothelin antagonists selective for the ET_A receptor. *Life Sci.* **1992**, *50*, 247–255.

- (14) Kikuchi, T.; Ohtaki, T.; Kawata, A.; Imada, T.; Asami, T.; Masuda, Y.; Sugo, T.; Kusumoto, K.; Kubo, K.; Watanabe, T.; Wakimasu, M.; Fujino, M. Cyclic hexapeptide endothelin receptor antagonists highly potent for both receptor subtypes ET_A and ET_B. *Biochem. Biophys. Res. Commun.* **1994**, *200*, 1708–1712.

- (15) Iqbal, J.; Sanghi, R.; Das, S. K. Endothelin receptor antagonists: an overview of their synthesis and structure-activity relationship. *Mini-Rev. Med. Chem.* **2005**, *5*, 381–408.

- (16) Cardillo, G.; Gentilucci, L.; Tolomelli, A.; Spinoso, R.; Calienni, M.; Qasem, A. R.; Spampinato, S. Synthesis and evaluation of the affinity toward μ -opioid receptors of atypical, lipophilic ligands based on the sequence c[-Tyr-Pro-Trp-Phe-Gly-]. *J. Med. Chem.* **2004**, *47*, 5198–5203.

- (17) Gentilucci, L.; Squassabia, F.; Demarco, R.; Artali, R.; Cardillo, G.; Tolomelli, A.; Spampinato, S.; Bedini, A. Investigation of the interaction between the atypical agonist c[YpwFG] and MOR. *FEBS J.* **2008**, *275*, 2315–2337.

- (18) Veber, D. F.; Freidinger, R. M.; Perlow, D. S.; Paleveda, W. J. Jr.; Holly, F. W.; Strachan, R. G.; Nutt, R. F.; Arison, B. H.; Homnick, C.; Randall, W. C.; Glitzer, M. S.; Saperstein, R.; Hirschmann, R. A potent cyclic hexapeptide analogue of somatostatin. *Nature* **1981**, *292*, 55–58.

- (19) Veber, D. F.; Saperstein, R.; Nutt, R. F.; Freidinger, R. M.; Brady, S. F.; Curley, P.; Perlow, D. S.; Paleveda, W. J.; Colton, C. D.; Zacchei, A. G.; Tocco, D. J.; Hoff, D. R.; Vandlen, R. L.; Gerich, J. E.; Hall, L.; Mandarino, L.; Cordes, E. H.; Anderson, P. S.; Hirschmann, R. A super active cyclic hexapeptide analog of somatostatin. *Life Sci.* **1984**, *34*, 1371–1378.

- (20) Fujii, N.; Oishi, S.; Hiramatsu, K.; Araki, T.; Ueda, S.; Tamamura, H.; Otaka, A.; Kusano, S.; Terakubo, S.; Nakashima, H.; Broach, J. A.; Trent, J. O.; Wang, Z.; Peiper, S. C. Molecular-size reduction of a potent CXCR4-chemokine antagonist using orthogonal combination of conformation- and sequence-based libraries. *Angew. Chem., Int. Ed.* **2003**, *42*, 3251–3253.
- (21) Inokuchi, E.; Oishi, S.; Kubo, T.; Ohno, H.; Shimura, K.; Matsuoka, M.; Fujii, N. Potent CXCR4 antagonists containing amidine type peptide bond isosteres. *ACS Med. Chem. Lett.* **2011**, *2*, 477–480 and references therein.
- (22) Ueda, S.; Oishi, S.; Wang, Z.; Araki, T.; Tamamura, H.; Cluzeau, J.; Ohno, H.; Kusano, S.; Nakashima, H.; Trent, J. O.; Peiper, S. C.; Fujii, N. Structure-activity relationships of cyclic peptide-based chemokine receptor CXCR4 antagonists: disclosing the importance of side-chain and backbone functionalities. *J. Med. Chem.* **2007**, *50*, 192–198.
- (23) Hann, M. M.; Sammes, P. G.; Kennewell, P. D.; Taylor, J. B. On double bond isosteres of the peptide bond; an enkephalin analogue. *J. Chem. Soc., Chem. Commun.* **1980**, 234–235.
- (24) Hann, M. M.; Sammes, P. G.; Kennewell, P. D.; Taylor, J. B. On the double bond isostere of the peptide bond: preparation of an enkephalin analogue. *J. Chem. Soc., Perkin. Trans. 1* **1982**, 307–314.
- (25) Christos, T. E.; Arvanitis, A.; Cain, G. A.; Johnson, A. L.; Pottorf, R. S.; Tam, S. W.; Schmidt, W. K. Stable isosteres of neurotensin C-terminal pentapeptides derived by modification of the amide function. *Bioorg. Med. Chem. Lett.* **1993**, *3*, 1035–1040.
- (26) Wipf, P.; Henninger, T. C.; Geib, S. J. Methyl- and (trifluoromethyl)alkene peptide isosteres: synthesis and evaluation of their potential as β -turn promoters and peptide mimetics. *J. Org. Chem.* **1998**, *63*, 6088–6089.
- (27) Xiao, J.; Weisblum, B.; Wipf, P. Trisubstituted (*E*)-alkene dipeptide isosteres as β -turn promoters in the gramicidin S cyclodecapeptide scaffold. *Org. Lett.* **2006**, *8*, 4731–4734.
- (28) Oishi, S.; Miyamoto, K.; Niida, A.; Yamamoto, M.; Ajito, K.; Tamamura, H.; Otaka, A.; Kuroda, Y.; Asai, A.; Fujii, N. Application of tri- and tetrasubstituted alkene dipeptide mimetics to conformational studies of cyclic RGD peptides. *Tetrahedron* **2006**, *62*, 1416–1424.
- (29) Narumi, T.; Tomita, K.; Inokuchi, E.; Kobayashi, K.; Oishi, S.; Ohno, H.; Fujii, N. Diastereoselective synthesis of highly functionalized fluoroalkene dipeptide isosteres and its application to Fmoc-based solid-phase synthesis of a cyclic pentapeptide mimetic. *Tetrahedron* **2008**, *64*, 4332–4346.
- (30) Narumi, T.; Hayashi, R.; Tomita, K.; Kobayashi, K.; Tanahara, N.; Ohno, H.; Naito, T.; Kodama, E.; Matsuoka, M.; Oishi, S.; Fujii, N. Synthesis and biological evaluation of selective CXCR4 antagonists containing alkene dipeptide isosteres. *Org. Biomol. Chem.* **2010**, *8*, 616–621.
- (31) Ibuka, T.; Habashita, H.; Funakoshi, S.; Fujii, N.; Oguchi, Y.; Uyehara, T.; Yamamoto, Y. Highly selective synthesis of (*E*)-alkene isosteric dipeptides with high optical purity via $\text{RCu}(\text{CN})\text{Li}\cdot\text{BF}_3$ mediated reaction. *Angew. Chem., Int. Ed. Engl.* **1990**, *29*, 801–803.
- (32) Oishi, S.; Niida, A.; Kamano, T.; Odagaki, Y.; Tamamura, H.; Otaka, A.; Hamanaka, N.; Fujii, N. Diastereoselective synthesis of $\psi[(E)\text{-CMe}=\text{CH}]$ - and $\psi[(E)\text{-CMe}=\text{CMe}]$ -type dipeptide isosteres based on organocopper-mediated *anti*- $\text{S}_{\text{N}}2'$ reaction. *Org. Lett.* **2002**, *4*, 1055–1058.
- (33) Oishi, S.; Niida, A.; Kamano, T.; Miwa, Y.; Taga, T.; Odagaki, Y.; Hamanaka, N.; Yamamoto, M.; Ajito, K.; Tamamura, H.; Otaka, A.; Fujii, N. Regio- and stereoselective ring-opening of chiral 1,3-oxazolidin-2-one derivatives by organocopper reagents provides novel access to di-, tri- and tetra-substituted alkene dipeptide isosteres. *J. Chem. Soc., Perkin Trans. 1* **2002**, 1786–1793.
- (34) Ando, K. Highly selective synthesis of *Z*-unsaturated esters by using new Horner–Emmons reagents, ethyl (diarylphosphono)-acetates. *J. Org. Chem.* **1997**, *62*, 1934–1939.
- (35) Yu, J. S.; Kleckley, T. S.; Wiemer, D. F. Synthesis of farnesol isomers via a modified Wittig procedure. *Org. Lett.* **2005**, *7*, 4803–4806.
- (36) Peterson, D. J. A carbonyl olefination reaction using silyl-substituted organometallic compounds. *J. Org. Chem.* **1968**, *33*, 780–784.
- (37) Hartzell, S. L.; Sullivan, D. F.; Rathke, M. W. Reaction of lithio *tert*-butyl trimethylsilylacetate with aldehydes and ketones. A synthesis of α,β -unsaturated esters. *Tetrahedron Lett.* **1974**, *15*, 1403–1406.
- (38) Våbenø, J.; Nikiforovich, G. V.; Marshall, G. R. Insight into the binding mode for cyclopentapeptide antagonists of the CXCR4 receptor. *Chem. Biol. Drug Des.* **2006**, *67*, 346–354.
- (39) Våbenø, J.; Nikiforovich, G. V.; Marshall, G. R. A minimalistic 3D pharmacophore model for cyclopentapeptide CXCR4 antagonists. *Biopolymers* **2006**, *84*, 459–471.
- (40) Demmer, O.; Dijkgraaf, I.; Schumacher, U.; Marinelli, L.; Cosconati, S.; Gourni, E.; Wester, H. J.; Kessler, H. Design, synthesis, and functionalization of dimeric peptides targeting chemokine receptor CXCR4. *J. Med. Chem.* **2011**, *54*, 7648–7662.
- (41) Yoshikawa, Y.; Kobayashi, K.; Oishi, S.; Fujii, N.; Furuya, T. Molecular modeling study of cyclic pentapeptide CXCR4 antagonists: new insight into CXCR4-FC131 interactions. *Bioorg. Med. Chem. Lett.* **2012**, *22*, 2146–2150.
- (42) Wu, B.; Chien, E. Y. T.; Mol, C. D.; Fenalti, G.; Liu, W.; Katritch, V.; Abagyan, R.; Brooun, A.; Wells, P.; Bi, F. C.; Hamel, D. J.; Kuhn, P.; Handel, T. M.; Cherezov, V.; Stevens, R. C. Structure of the CXCR4 chemokine GPCR with small-molecule and cyclic peptide antagonists. *Science* **2010**, *330*, 1066–1071.
- (43) Molecular Operating Environment (MOE), Chemical Computing Group Inc., Montreal, QC, Canada.

Peptide and peptidomimetic ligands for CXC chemokine receptor 4 (CXCR4)[†]

Shinya Oishi and Nobutaka Fujii*

Received 14th January 2012, Accepted 16th March 2012

DOI: 10.1039/c2ob25107h

The development of novel peptide and peptidomimetic ligands for the CXC chemokine receptor 4 (CXCR4) as therapeutic agents for HIV-1 infection, cancer, and immune system diseases has grown over the last decade. In this perspective article, the design of CXCR4 agonists and antagonists from endogenous stromal cell-derived factor-1 (SDF-1)/CXCL12 and horseshoe crab-derived antimicrobial peptides and their therapeutic and diagnostic applications are described.

1. Introduction

CXC chemokine receptor 4 (CXCR4) is a G protein-coupled receptor (GPCR) of stromal cell-derived factor-1 (SDF-1)/CXCL12,¹ which has been implicated in a number of developmental and physiological processes including directed migrations of stem cells and immune cells.² In terms of a target molecule in drug discovery, CXCR4 is well-known to be a co-receptor for human immunodeficiency virus type-1 (HIV-1) infection into T cells.³ Compounds exerting inhibitory activity on the gp120–CXCR4 interaction have been considered as promising anti-HIV agents, because attachment of envelope glycoprotein gp120 of HIV-1 to CD4 and CXCR4 on the host cell surface is a critical step leading to membrane fusion and virus entry.

The organ-specific metastasis of breast cancer cells was first documented in 2001.⁴ It was demonstrated that CXCR4-expressing cancer cells migrate based on the magnitude of the concentration gradient of SDF-1 from the distant metastatic lesions.⁴ During the last decade, the clinical importance and therapeutic implications of the pivotal SDF-1–CXCR4 interaction in cancer biology including progression, metastasis and angiogenesis, have been revealed.⁵ CXCR4 antagonists are expected to behave as anti-tumor and anti-metastatic agents in cancer chemotherapy.⁶

To date, a number of CXCR4 ligands (agonists and antagonists) have been reported. The most representative agent is the small-molecule CXCR4 antagonist, plerixafor (Mozobil, AMD3100), which was approved for clinical use in the United States and in Europe in 2008 and 2009, respectively.⁷ Although plerixafor was originally developed as an anti-HIV agent, it is

now employed for the mobilization of hematopoietic stem cells (HSC) into the peripheral blood in combination with granulocyte colony-stimulating factor (G-CSF). Autologous transplantation of HSC facilitates the restoration of normal hematopoietic function in patients with non-Hodgkin's lymphoma and multiple myeloma after receiving high-dose chemotherapy. Several other peptide and non-peptide CXCR4 antagonists have also been reported to be inhibitory compounds for CXCR4-mediated HIV-1 infection.⁸

In this review article, we focus on the development of peptide and peptidomimetic CXCR4 ligands, which are mainly derivatives of horseshoe crab-derived antimicrobial peptides or the endogenous SDF-1 sequence. The application of these ligands as therapeutic and diagnostic agents for immune system diseases and oncologic conditions are also introduced.

2. CXCR4 antagonists derived from self-defense peptides of horseshoe crabs

2.1. Identification of T22 and its derivatives: the first generation of CXCR4 antagonists

In 1991, Morimoto *et al.* reported that tachyplesin I showed antiviral activity against HIV-1, vesicular stomatitis virus and influenza A virus.⁹ Subsequently, the anti-HIV activities of the isopeptides of tachyplesin I such as tachyplesin II and polyphemusins I and II, which were isolated from the hemocytes of horseshoe crabs (*Tachyplesus tridentatus* and *Limulus polyphemus*),¹⁰ were reported (Table 1).¹¹ These antimicrobial peptides contain two disulfide bridges which stabilize the antiparallel β -sheet structure connected by a β -turn.

T22 ([Tyr^{5,12},Lys⁷]-polyphemusins II) is a first-generation peptide of highly potent anti-HIV peptides that was designed from horseshoe crab-derived natural product peptides.^{11,12} On the basis of the highly cationic sequences of tachyplesins and polyphemusins, more than twenty analogs were synthesized and

Graduate School of Pharmaceutical Sciences, Kyoto University, Sakyo-ku, Kyoto 606-8501, Japan. E-mail: nfujii@pharm.kyoto-u.ac.jp; Fax: +81-75-753-4570; Tel: +81-75-753-4551

[†]This article is part of the *Organic & Biomolecular Chemistry* 10th Anniversary issue.

Table 1 Polyphemusin II-derived CXCR4 antagonists

| Peptide | Sequence ^a | Ref. |
|-----------------|---|-------|
| Tachyplesin I | <i>H</i> -KWC ¹ FRVC ² YRGC ² YRRC ¹ R-NH ₂ (C ¹ -C ¹ /C ² -C ² bridged) | 9 |
| Polyphemusin II | <i>H</i> -RRWC ¹ FRVC ² YKGF ² YRKC ¹ R-NH ₂ (C ¹ -C ¹ /C ² -C ² bridged) | 11 |
| T22 | <i>H</i> -RRWC ¹ YRKC ² YKGYC ² YRKC ¹ R-NH ₂ (C ¹ -C ¹ /C ² -C ² bridged) | 11,12 |
| TW70 | <i>H</i> -RRWCYRkkPYRKC ² R-NH ₂ (C-C bridged) | 22 |
| T134 | <i>H</i> -RRWCYRkkPYRX ² CR-OH (C-C bridged) | 24 |
| T140 | <i>H</i> -RRX ¹ CYRkkPYRX ² CR-OH (C-C bridged) | 26 |
| TN14003 | <i>H</i> -RRX ¹ CYX ² KkPYRX ² CR-NH ₂ (C-C bridged) | 34 |
| TC14012 | <i>H</i> -RRX ¹ CYX ² Kx ² PYRX ² CR-NH ₂ (C-C bridged) | 34 |
| TE14011 | <i>H</i> -RRX ¹ CYX ² KePYRX ² CR-NH ₂ (C-C bridged) | 35 |
| TF14016 | 4FB-RRX ¹ CYX ² KkPYRX ² CR-NH ₂ (C-C bridged) | 36 |
| FC131 | cyclo(-D-Tyr-Arg-Arg-Nal-Gly-) [Fig. 2] | 47 |
| FC122 | cyclo(-D-Tyr-D-MeArg-Arg-Nal-Gly-) [Fig. 2] | 48c |
| FCA004 | cyclo(-D-Tyr-Arg-Arg-Nal-ψ[C(=NH)-NH]-Gly-) [Fig. 2] | 51 |

^a X¹: L-3-(2-naphthyl)alanine; X²: L-citrulline; x²: D-citrulline; 4FB: 4-fluorobenzoyl; Nal: L-3-(2-naphthyl)alanine.

evaluated. Among the peptides, T22 showed excellent anti-HIV activity with a high selectivity index. The solution structure of T22 takes an anti-parallel β -sheet structure, which is similar to that of tachyplesin I.¹³ Given the attractive lead-like properties of the T22 peptide for anti-HIV agents, intensive structural analysis and structure-activity relationship (SAR) studies have been conducted. The stereochemically antipodal peptide of T22 (all-D-isomers) was 8.5-fold less potent in comparison with the parent T22. Peptides with retro- and retro/inverse-sequences were much less potent, suggesting that the target molecule(s) of T22 should be the chiral components on the host cells or virus.¹⁴ SAR study of T22 demonstrated that the two disulfide bridges and two repeated Tyr-Arg-Lys (Y-R-K) motifs are indispensable to the anti-HIV activity of T22.¹⁵ The disulfide bonds are substituted with a Zn(II) ion to form a tetracoordinate complex with equipotent anti-HIV activity.¹⁶ Substitution of Trp³ with 3-(2-naphthyl)alanine (Nal) in T22 led to the most potent T22 analogue.^{15b}

The target molecule of T22 for the anti-HIV activity was originally thought to be cell surface CD4 on T-cells or viral gp120. Weeks *et al.* reported that a phorbol ester stimulates the attachment of lymphocytes to T22, suggesting the presence of a cell surface receptor for T22.¹⁷ In contrast, CD4-negative HeLa and U87MG cells did not bind to T22.¹⁸ In an affinity chromatography experiment, a 55 kDa molecule, which was captured using a T22 affinity column, was detected with anti-CD4 antibody by western blotting.¹⁸ Biosensor analysis by surface plasmon resonance also demonstrated that T22 binds to both immobilized CD4 and gp120 with the same affinity.¹⁹ It was subsequently revealed in 1997 that the anti-HIV activity of T22 was derived from CXCR4 binding.²⁰ T22 specifically inhibits the T-cell line-tropic (T-tropic) HIV-1 infection of cells expressing CXCR4 and CD4, whilst no inhibitory effect by T22 was observed against macrophage-tropic (M-tropic) HIV-1 infection of CCR5-expressing cells. T22 also inhibits SDF-1 α -induced Ca²⁺ mobilization, chemotaxis of peripheral blood mononuclear cells (PBMC) and migration of pancreatic cancer cell lines through binding to CXCR4.²¹

2.2. Design of T140 and its derivatives: the second generation of CXCR4 antagonists

In an attempt to reduce the molecular size of T22, a second generation of polyphemusin II-derived CXCR4 antagonist was

identified (Table 1).²² During the molecular design from T22, the outer disulfide bond, that is more conducive to the anti-parallel β -sheet structure and two repeats of indispensable Tyr-Arg-Lys (Y-R-K) sequences were retained to reproduce the potent anti-HIV activity. In addition, the β -turn moiety of T22 was stabilized using turn-stabilizing motifs, such as D-Lys-Pro or Pro-D-Lys sequences. TW70 (des-Cys^{8,13}, Tyr^{9,12}-[D-Lys¹⁰, Pro¹¹]-T22) was the first 14-residue CXCR4 antagonist, which showed bioactivity comparable to that of T22.²² Analysis by CD and NMR spectroscopies revealed that TW70 maintains an antiparallel β -sheet structure with a type II' β -turn motif.²³

Following on from the milestone discovery of TW70, intensive SAR studies of 14-residue β -sheet peptides have been carried out. The first approach taken was for the purpose of designing less cytotoxic analogues.²⁴ TW70 contains a number of basic amino acid residues (five Arg and three Lys residues) which may be related to the high level of collateral cytotoxicity. To decrease the number of these positively charged functional groups, substitutions with glutamic acid (Glu) and citrulline (Cit) were attempted. From a collection of 20 peptides designed, T134 ([Cit¹²]-TW70) showed more potent anti-HIV activity and significantly less cytotoxicity [selectivity index (SI) = 34 000] when compared with T22 and TW70.²⁴ Of interest, T134 is effective even against drug-resistant HIV strains which were non-responsive to the small-molecule CXCR4 antagonist AMD3100.²⁵

T140 is a key 14-residue peptide CXCR4 antagonist that was obtained by lead optimization of TW70 derivatives,²⁶ in which the Trp³ of T134 was substituted with Nal, in a modification similar to that of T22.^{15b} The significant contribution of Nal³ to the potent bioactivity was demonstrated by the subsequent SAR study at the 3-position of T140 of inhibitory activity on SDF-1-induced Ca²⁺ mobilization and anti-HIV activity.²⁷ Although both T22 and T140 upregulate the provirus transcription level driven by the HIV-1 long terminal repeat (LTR) promoter,²⁸ the binding of anti-CXCR4 monoclonal antibody 12G5 was more efficiently inhibited by T140 than by T22, suggesting that the potent anti-HIV activity of T140 was derived from the enhanced binding affinity to CXCR4.²⁹ It is noteworthy that T140 is an inverse agonist for a constitutively active mutant (CAM) of CXCR4, whilst AMD3100 is a weak partial agonist.³⁰

Alanine scanning experiments of T140 identified Arg², Nal³, Tyr⁵, Arg¹⁴ residues as indispensable to the bioactivity.³¹ An NMR-based conformational study suggested that these intrinsic residues exist in close proximity to a disulfide bridge.³² In contrast, modifications at the β -turn moiety of T140 with peptide backbone mimetics had little effect on CXCR4 binding and anti-HIV activity.³³ In light of this information, further optimization of T140 was conducted using two separate approaches. The first approach was focused on the design of less cytotoxic and biologically stable analogues. C-terminally amidated T140 analogues were designed, in which one or two Arg residue(s) were substituted with Cit to further reduce the cytotoxicity, because the C-terminal Arg14 in T140 was gradually cleaved in serum.³⁴ TN14003 ([Cit⁶]-T140 with the C-terminal amide) and TC14012 ([Cit⁶,D-Cit⁸]-T140 with the C-terminal amide) showed high selectivity indexes (SIs) and complete stability in serum.³⁴ Substitution of D-Lys⁸ with the negatively charged D-Glu⁸ also effectively enhanced the anti-HIV activity whilst lowering cytotoxicity to provide TE14011 ([Cit⁶,D-Glu⁸]-T140 with the C-terminal amide).³⁵ The second approach was the attachment of an additional functional group onto the T140 N-terminus. An SAR study using a wide variety of acyl groups revealed that the 4-fluorobenzoyl group constituted a novel pharmacophore for T140-based CXCR4 antagonists, providing the most potent antagonist, TF14016 (4-fluorobenzoyl-TN14003), with subnanomolar inhibition of the binding of SDF-1 to CXCR4.³⁶

T140 and related peptides have been further researched for applications in a number of basic biology and drug discovery approaches including effective inhibition of SDF-1-induced cell migration of breast and prostate cancers,³⁷ prevention of pulmonary metastasis of melanoma cells,³⁸ and suppression of rheumatoid arthritis.³⁹ More efficient mobilization of stem cells from bone marrow was reported by TF14016 compared with plerixafor/AMD3100.⁴⁰ It was also demonstrated that T140 serves as a cargo molecule carrying anti-HIV agents such as azidothymidine (AZT) to the target cells.⁴¹ In a separate experiment, Ichiyama *et al.* reported that small-molecule KRH-1636, which mimics the N-terminal motif of T140, is a potent and selective CXCR4 antagonist with high anti-HIV activity.⁴²

Prior to the recent publication of X-ray crystallography analysis of CXCR4 (Fig. 1),⁴³ there had been several attempts made to estimate the binding mode of T140 derivatives. For example, intensive point mutation experiments of CXCR4 identified the residues responsible for ligand binding.⁴⁴ It was demonstrated in fusion assays using the HIV-1 89.6 envelope glycoprotein, that conversion of Asp171, Arg188, Tyr190, Gly207, or Asp262 to Ala led to the loss of T140 bioactivity. This suggested that these five residues were critical for T140 binding. On the basis of these experiments, a docking model was created, in which the key T140 residues all interacted with the residues in the N-terminus, the 4th and 5th transmembrane domains (TM4 and TM5), extracellular loop 2 (EL2) and EL3 of CXCR4.

To date, two experiments have been reported using a photolabeling approach to determine the CXCR4 binding sites of T140. Using photoaffinity probes ¹²⁵I-[Bpa⁵]-T140 and ¹²⁵I-[Bpa¹⁰]-T140 [*p*-benzoyl-L-phenylalanine (Bpa)], a fragment of Lys154-Glu179 in CXCR4 4TM was identified as the interactive site of T140.⁴⁵ In contrast, Grunbeck *et al.* employed several Bpa-containing CXCR4 mutants, which were constructed using stop

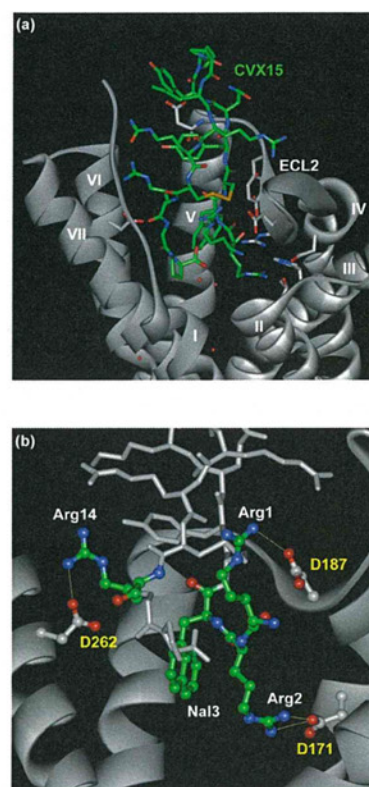


Fig. 1 Crystal structure of CXCR4 in complex with a T140 analogue peptide, CVX15 (PDB code: 3OE0). (a) CVX15–CXCR4 interaction in the receptor pocket. (b) Charge interactions between CVX15 and CXCR4.

codon suppression technology. From the eight positions substituted, Phe189 in EL2 was identified as the binding site of T140.⁴⁶

In a recent report on the crystal structure of CXCR4 in complex with a T140 analogue peptide, CVX15, the binding mode of the polyphemusin II-derived CXCR4 antagonists was clearly revealed (Fig. 1, PDB code: 3OE0).⁴³ CVX15 was bound to the receptor with the key residues (Arg², Nal³, Tyr⁵ and Arg¹⁴) inside the receptor pocket and the β -turn site exposed to the extracellular milieu. The Arg¹, Arg² and Arg¹⁴ residues in CVX15 interacted with Asp187, Asp171 and Asp262, respectively, and the hydrophobic group of CVX15 Nal³ was anchored in the hydrophobic region of TM5.

2.3. Identification of a novel cyclic pentapeptide scaffold for CXCR4 antagonists: the third generation of antagonists

FC131 [cyclo(-D-Tyr-Arg-Arg-Nal-Gly-)] is a cyclic pentapeptide-based CXCR4 antagonist, which was developed using a molecular-size reduction approach (Table 1). Using the four indispensable residues (Tyr, Nal, and two Arg) in T140 and an additional Gly linker, bioevaluation of two cyclic pentapeptide libraries led to the identification of an anti-HIV peptide with CXCR4 antagonism, which was equipotent to the parent T140.⁴⁷ Further SAR studies of cyclic pentapeptides including alanine-scanning, *N*-methyl amino acid scanning, optimization of amino

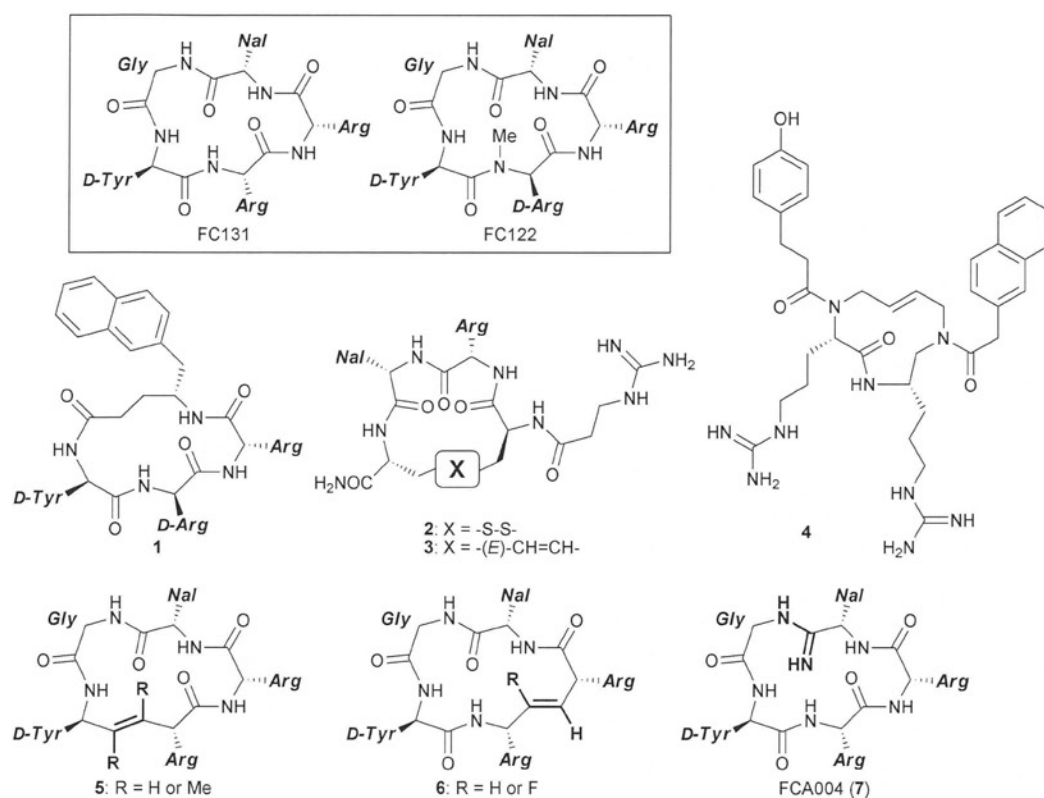


Fig. 2 Structure of peptidomimetic analogues of FC131.

acids and design of retro-inverso sequence peptides suggested the indispensable side-chain functional groups and potential bioactive conformations of FC131.⁴⁸ FC122 [cyclo(-D-Tyr-D-MeArg-Arg-Nal-Gly-)] is the most potent cyclic pentapeptide-based CXCR4 antagonist.^{48c} Recently, the *in vivo* inhibitory effects on the growth of GH3 somatotrope tumor cell xenografts by one of the analogous peptides FC092 ([D-Arg²]-FC131) was reported.⁴⁹

Several peptidomimetic analogues of FC131 have been reported (Fig. 2).⁵⁰ Replacements of the dipeptide unit (Nal-Gly) with a γ -amino acid **1**, disulfide bridge **2** and olefin bridge **3** have provided novel scaffold structures.^{50a} Cluzeau *et al.* reported 11-membered ring core peptidomimetic **4** with the key functional groups, which were prepared by a divergent methodology from L- and D-glutamic acids and by ring closing metathesis.^{50c} Modification of FC131 with alkene-type dipeptide isosteres (**5** and **6**) has also been conducted to investigate the possible hydrogen bonding contributions of each peptide bond.^{50d-g} Some of these FC131 derivatives with the modification to the peptide backbone showed high to moderate CXCR4 antagonistic activity, although the approaches failed to improve the bioactivity of FC131 derivatives. In contrast, amidine-type peptide bond mimetics significantly improved the CXCR4 binding and anti-HIV activities of FC131 derivatives.⁵¹ On the basis of the highly basic properties of T140 derivatives and the known small-molecule CXCR4 antagonists, each peptide bond of the FC131 backbone was substituted with a planar and basic amidine unit to provide potent FC131 analogues. The best

analogue FCA004 [cyclo(-D-Tyr-Arg-Arg-Nal- ψ [C(=NH)-NH]-Gly-)] **7** exhibited a 30-fold increase in potency compared with the parent FC131.

An alternative approach for FC131-based antagonists is the design of bivalent ligands with an appropriate linker against potential dimerized CXCR4 receptors.⁵² Tanaka *et al.* reported the design of dimeric FC131 derivatives with a rigid poly(L-proline) linker to determine the distance between the two ligand binding sites of the CXCR4 dimer. When the possible linker length was in the range of 5.5–6.5 nm, the maximum increase in the binding affinity to CXCR4 was observed.^{52a} In a further example of dimeric FC131, derivatives with a shorter spacer were designed based on the known bivalent small-molecule CXCR4 antagonists, in which diacids with a variety of carbohydrate linkers were employed to bridge the ornithine side-chains of the FC131 analogue ([D-MeOrn²]-FC131). Dimer peptides of [D-MeOrn²]-FC131 with a 5–10 carbon atom spacer showed similarly potent bioactivity.^{52b}

There have been several recent reports describing the pharmacophore and binding models of FC131 derivatives using homology models⁵³ and crystal structures^{50g,52b,54} of CXCR4. Demmer *et al.* reported that [D-MeOrn²]-FC131 had a similar binding mode to that of CVX15, in which two basic groups from MeOrn² and Arg³ residues interact with the Asp187 and Asp171 residues of CXCR4, respectively.^{52b} We also revealed the binding modes of FC131 and FC122 by NMR analysis and molecular modeling studies (Fig. 3).^{50g,54} The hydroxyl group of D-Tyr¹ forms a hydrogen bond with Tyr45. The L-Arg² side

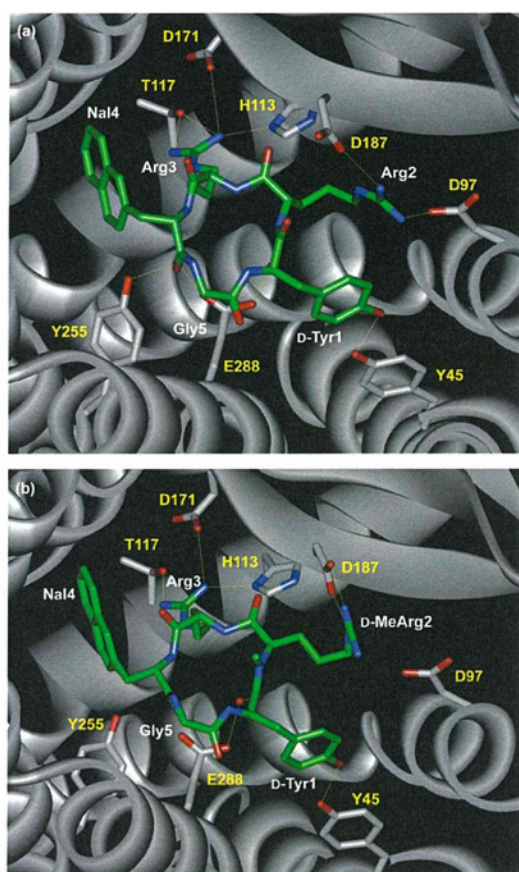


Fig. 3 Binding modes of FC131 (a) and FC122 (b) with CXCR4.

chain forms polar interactions with both Asp97 and Asp187 in CXCR4, and the L-Arg³ side-chain interacts with His113, Thr117, and Asp171 in CXCR4. Glu288 in CXCR4 is involved in the FC131 binding by hydrogen bond networks *via* two water molecules. The L-Nal⁴ carbonyl oxygen is involved in a hydrogen bond network including Tyr255 and Glu288 side chains *via* a crystal water molecule, and the backbone NH of L-Arg² makes another hydrogen bond network with CXCR4 Glu288 through a water molecule. FC122 binds with CXCR4 by an alternative binding mode with the flipped D-Tyr¹-D-MeArg² peptide bond, which was obtained on the basis of the characteristic binding mode of the congeneric peptidomimetics.^{50g} The D-Tyr¹ carbonyl oxygen in FC122 formed a hydrogen bond network *via* a water molecule.

2.4. β -Hairpin peptidomimetic CXCR4 antagonists

DeMarco *et al.* reported the identification of potent β -hairpin CXCR4 antagonists⁵⁵ using a macrocyclic peptide template of β -hairpin protein epitope mimetics (PEM).⁵⁶ In the β -hairpin PEM design, the template D-Pro-L-Pro dipeptide can stabilize a type-II' β -turn substructure. In addition, a disulfide bridge between two cysteine residues in each strand contributed to the stabilization of the β -hairpin conformation of the macrocyclic peptide. The loop sequence from the protein/peptide of interest could be incorporated into the other residues.

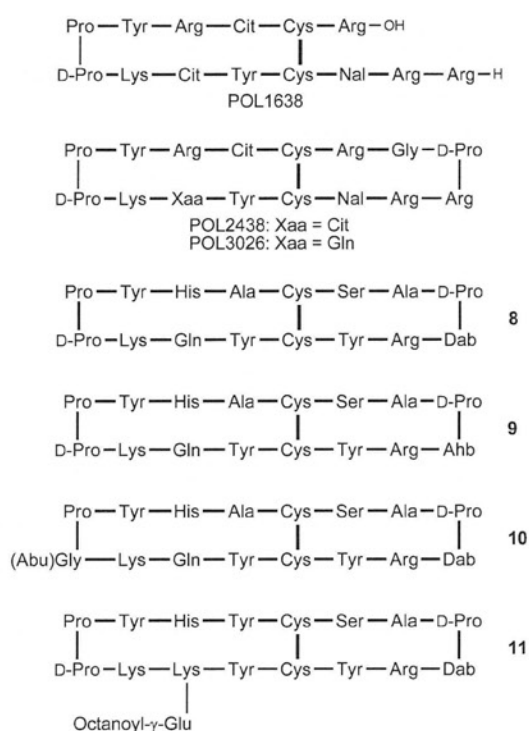


Fig. 4 Structures of β -hairpin peptidomimetic CXCR4 antagonists. Abbreviations: Nal: L-3-(2-naphthyl)alanine; Cit: L-citrulline; Dab: L-2,4-diaminobutyric acid; Ahb: (S)-4-amino-2-hydroxybutyric acid; (Abu)Gly: N-(4-amino-n-butyl)glycine; Lac: lactic acid.

In the first step to design β -hairpin PEM molecules for CXCR4 antagonists from T140 derivatives, D-Cit-L-Pro dipeptide in TC14011 was substituted with a D-Pro-L-Pro peptide template to provide an equipotent peptide POL1638 (Fig. 4). Development of the appropriate linker unit for macrocyclization was then explored using a peptidomimetic library. A Gly-D-Pro dipeptide linkage between the N- and C-termini of POL1638 gave the bicyclic peptides, POL2438 and POL3026, with a ten-fold increase in potency. The macrocyclic structure of both peptides resulted in higher plasma and metabolic stabilities. *In vivo* pharmacokinetic experiments on POL3026 demonstrated an excellent bioavailability profile following subcutaneous administration. POL2438 and POL3026 inhibited HIV replication for a broad panel of X4 and dualtropic strains and POL3026 prevented the emergence of X4 variants from an R5 strain.^{56a,57} The specificity for CXCR4 was verified by the inhibitory effect on staining by monoclonal antibodies for the potential receptors. As described above, the binding modes of CVX15 with CXCR4 were determined recently by X-ray crystallography (Fig. 1).⁴³ The peptide ligand CVX15 in the complex with CXCR4 is an open-chain analogue of POL3026.

The alternative CXCR4 antagonists with a β -hairpin peptidomimetic scaffold were reported by the researchers at Polyphor and the University of Zurich (Fig. 4).⁵⁸ The 16-residue bicyclic peptides **8** exhibited a highly potent inhibitory effect against SDF-1-mediated Ca²⁺ mobilization. Depsipeptides, including lactic acid (Lac) and (S)-4-amino-2-hydroxybutyric acid (Ahb) **9** also showed potent CXCR4 antagonism with good plasma stability.⁵⁹ Optimization of the D-Pro-L-Pro dipeptide template